Asociación Argentina
de Mecánica Computacional

Mecánica Computacional Vol XXVI pp.3745-3756
Sergio A. Elaskar, Elvio A. Pilotta, Germán A. Torres (Eds.)
Córdoba, Argentina, Octubre 2007

FLOW PATTERN EFFECT ON THE INITIAL SHAPE OF THE ATHEROMA

Valeria C. Gessaghi[a], Marcelo Raschi[b], Carlos A. Perazzo[c], Axel E. Larreteguy[b]

[a]Facultad de Ingeniería, Universidad Nacional de La Pampa,L6360AOJ.General Pico, La Pampa, Argentina, gessaghi@ing.unlpam.edu.ar
[b] Facultad de Ingeniería y Ciencias Exactas, y Centro de Estudios Avanzados, Universidad Argentina de la Empresa,C1073AAO Ciudad Autónoma de Buenos Aires, Argentina , mraschi@uade.edu.ar, alarreteguy@uade.edu.ar
[c]Facultad de Ingeniería y Ciencias Exactas y Naturales, Universidad Favaloro,C1078AAI,Ciudad Autónoma de Buenos Aires, Argentina, perazzo@favaloro.edu.ar y CONICET

Keywords: Atherosclerosis, atheroma, hemodynamics.

Abstract. Atherosclerosis is the first cause of death in the first world countries nowadays and it will also become one of the firsts in the developing countries. It is a vascular disease that affects medium and great size arteries and it could partially or totally obstruct blood flow through them. The lack of blood supply to an organ implies the lack of oxygen and this could mean its temporary mal functioning (ischemia) or the death of the tissue (infarct). This disease implies the formation of plaques called atheromas, which grow in the arterial wall due to accumulation of fat, cholesterol, cell debris, calcium and smooth muscle cells. Since late seventies it has been hypothesized that hemodynamic forces over the endothelium, the innermost layer of arteries, are very important to the formation and development of atheromas. These hypotheses suggest that atheromas form in regions of complex flow patterns, such as bifurcations or regions of marked curvature, where recirculation and secondary flow develops. Together with flow patterns, blood pressure and cholesterol concentration in blood are other known factors that influence the development of the atherosclerotic plaques. The carotid bifurcation in the carotid artery has received and continues to receive a lot of attention for it supplies blood to some parts of the brain. Atheromas that develop in this bifurcation may cause a stroke, which is one of the major causes of death. In previous works we have shown a model of the formation and initial growth of these plaques. In the present work we use a slight modification of this model, combined with Finite Volume simulations of the blood flow through the artery, to predict the time evolution of the shape of an atheroma in the human carotid bifurcation.

1 INTRODUCTION

Atherosclerosis is an inflammatory disease that affects large and medium-sized arteries (Ross, 1999). The atherosclerotic lesion, *atheroma*, is a focal thickening of the innermost layer of the artery wall, called intima. These lesions consist mainly of accumulation of lipids, endothelial and vascular smooth muscle cells (SMC), connective tissue and debris (Berliner et al., 1995). The evolution of the atheroma is not constant in time; on the contrary it can have both chronic and acute manifestations. Few human diseases have longer incubation period than atherosclerosis, which begins to affect arteries during the second ant third decades of life and yet, its symptoms do not appear until several decades later (Braunwald et al., 2001). The atheroma will evolve causing a temporary or permanent lack of blood and oxygen supply to some organ, which can result in its malfunction or the infarct of the organ tissue. These manifestations could be classified in three groups, based on the organ that affects: cerebrovascular disease, ischemic heart disease and peripheral vascular disease.

Despite the efforts done to reduce it, cardiovascular diseases continues to be the principal cause of deaths in North America, Europe and a big part of Asia, and is expected to be so in every country within the next two decades (AHA, 2003b, AHA, 2003a). This is the reason why, in the past few decades, there has been a big effort devoted to learn and understand its genesis and to find the main risk factors for the atherosclerotic disease (Jensen-Urstad et al., 1999, Altman, 2003, Hinderliter and Caughey, 2003).

In the late 60´s and the early 70´s, the first theories about the focal nature of lesion initiation came to light (Fry, 1969, Caro et al., 1971). These theories proposed that the hemodynamic forces exerted by the blood flow on the artery wall, more specifically on the vascular wall endothelial layer, have a major influence on the location where the atherosclerotic plaques will develop. Researchers agree that atheromas develop in areas where there are complex flow patterns such as recirculation and/or secondary flows, which occur in arterial bifurcations, junctions or regions with marked curvature. The endothelium in these areas is subjected to low and oscillating shear stresses due to the flow patterns, which is thought to be the cause of the location of the plaques (Friedman and Giddens, 2005, Ku, 1997). However, there are different theories about why this is so. Some research focus their effort on studying the blood cholesterol transport to find out how its concentration at the wall on the lumen side varies with position (Ma et al., 1997, Rappitsch and Perktold, 1996), while others propose that there is a malfunction of the endothelium caused by these shear stresses and concentrate on looking for a dependence of the permeability of the endothelium on the shear stress (Hazel et al., 2003, Friedman and Ehrlich, 1975), while other try to model the cellular response to shear(Barakat, 2001, Barakat and Lieu, 2003).

Lately, there has also been a few works that simulated a coupled transport of low density lipoproteins (LDL) in blood and through the artery wall (Stangeby and Ethier, 2002, Sun et al., 2006). These works intend to predict the variation of the transendothelial LDL flux along the artery axial direction, as well as the LDL concentration in the wall, especially before and after the stenosis caused by the growing atheroma.

In spite of all the effort made to study this disease, specially the influence of the wall shear stress caused by the complex flow patterns, to the authors knowledge, there are no studies published that include the variation in the flow patterns caused by the growing atheroma in a complex arterial geometry such as the carotid bifurcation. This work presents simulations and analysis of the variation of the flow patterns in the carotid bifurcation as atheroma growths and the wall internal shape changes.

We apply a simple model for the plaque growth rate based on the accumulation of oxidized LDL in the artery wall (Gessaghi et al., 2006, Gessaghi et al., 2005), including a dependence

of the endothelial permeability on the shear stresses, as proposed by LaMack (LaMack et al., 2005), and on the LDL blood concentration, as proposed by Stangeby (Stangeby and Ethier, 2002). The simulations were made using a Finite Volume open source CFD toolbox, OpenFoam v1.4 (2007) and assuming a steady mean flow of blood, taken as an homogeneous and Newtonian fluid.

2 ATHEROSCLEROTIC PLAQUE GROWTH

2.1 Atherogenesis and plaque evolution

Although it is not known what is the major determinant for the initiation, it seems that the relevant factor that influence the LDL mass flux to the artery wall in these specific locations are the complex flow patterns developed due to bifurcations or high curvature regions (Rappitsch and Perktold, 1996). These seem to cause extracellular LDL accumulation, part of which suffers an oxidative reaction, LDLox. Another important event that is distinguished in the initiation of the atheroma is the leukocyte recruitment. Monocytes and T lymphocytes tend to accumulate in the early atherosclerotic lesion. The monocytes become macrophages in the artery wall and ingest the oxidized LDL turning into foam cells, commonly found in atheromas (Braunwald et al., 2001).

The evolution of the atheroma into more complex plaque, involves SMC migration and proliferation. On the other hand, it is the extracellular matrix rather than the cells themselves that makes up much of the volume of an advanced atherosclerotic plaque. The vascular smooth muscle cells produce this excessive extracellular matrix macromolecules, such as collagens and proteoglycans (Braunwald et al., 2001).

2.2 The model

A growth model presented previously (Gessaghi et al., 2006, Gessaghi et al., 2005) was modified to be used here. It is based on the concept of conservation of LDL mass, expressed as

$$\frac{DC_{LDL}}{Dt} = -\nabla . J_{LDL} + \dot{N}_{LDL} \quad , \tag{1}$$

where C_{LDL} is the concentration of LDL in the intima, J_{LDL} is the LDL flux vector and $\dot{N}_{LDL}$ is the consumption of LDL due only to the oxidative reaction, since all other reactions were neglected.

The LDL is mainly transported by the blood; therefore, all the convective and diffusion fluxes in the axial and tangential direction in the artery wall were neglected compared to the LDL flux that goes through the endothelium into the intima $\left(J_{LDL,in}\right)$. It was also assumed that this flux either goes through an oxidative reaction $\left(\dot{N}_{LDL}\right)$ or goes out of the wall to the media and the lymph system $\left(J_{LDL,out}\right)$ as equation 2 shows (here, e_0 is the intima initial thickness):

$$\frac{dC_{LDL}}{dt} \approx -\frac{J_{LDL,out} - J_{LDL,in}}{e_0} + \dot{N}_{LDL} = 0 \tag{2}$$

The endothelium is treated as a semi permeable membrane. The LDL that goes into the intima is driven by both a convective flux of plasma, J_v, and a diffusive flux proportional to

the transmembrane LDL concentration difference, ΔC_{LDL}. The model for these fluxes is shown in equations 3, known as the Kedem-Katchalsky equations (Kargol and Kargol, 2003)

$$J_v = L_p\left(\Delta p - \sigma\,\Delta\pi\right),$$
$$J_{LDL,in} = P_d\,\Delta C_{LDL} + \left(1-\sigma\right) J_v \bar{C}_{LDL}, \quad (3)$$

where L_p is the hydraulic conductivity of the endothelium, P_d is the endothelial permeability to LDL, σ is the endothelial reflection coefficient, Δp and $\Delta\pi$ are the transmembrane hydrodynamic and osmotic pressure differences, respectively, and $\bar{C}_{LDL}$ is the mean endothelial concentration (Michel and Curry, 1999). In this model, the transmembrane hydrodynamic pressure difference is assumed constant, Δp = 70 mmHg, and the osmotic pressure difference is calculated using the van´t Hoff´s formula,

$$\Delta\pi = \frac{R}{M_{LDL}} T \Delta C_{LDL},$$

where R = 8.3145 J/mol.K is the universal gas constant, MLDL is the LDL molecular weight and T is the solute temperature (i.e.: body temperature, 37 ºC). The reflection coefficient and the hydraulic conductivity where also assumed constant, σ = 0.9979 and L_p = 3x10-12 m $s^{-1}Pa^{-1}$ as found in the literature (Sun et al., 2006, Yang and Vafai, 2006).

The influence of the hemodynamic forces is represented by the dependence of the endothelial permeability of the wall shear stress, τ_w. Although it is not clear how is the shear stress sensed by the cell, there are a few models proposed in the literature (Rappitsch and Perktold, 1996, Friedman and Fry, 1993). The model adopted here for the endothelial permeability includes a dependence on the wall shear stress as proposed by LaMack et al. (2005), which assumes that the permeability depends on the absolute value of the wall shear stress, in the following way:

$$P_d = P_{d0}.e^{2.75\,C_{LDL},blood/C_0}\left|\tau_w\right|^{-0.11} \quad (4)$$

It also accounts for the influence of the LDL concentration in blood, $C_{LDL,blood}$, using a model proposed by Stangeby and Ethier (2002).

The constant P_{d0} = 1.15 *x* 10-11 Pa.m.s^{-1} was scaled so that the permeability is 2x10^{-10}m.s^{-1} at the inlet of the artery, which is considered a normal or reference value in the literature (Prosi et al., 2005) and C_0 is the LDL concentration in blood recommended by physicians, 1.2 kg LDL/m^3. The LDL concentration in blood was assumed constant in the circulation based on the relation between the Sherwood number,

$$Sh_d = \frac{h_{LDL}\,d}{D_{LDL}^{blood}},$$

that is the dimensionless mass transfer coefficient (calculated with the arterial diameter, d, the mass transport coefficient in blood, h_{LDL}, and the LDL diffusion coefficient in blood, D_{LDL}^{blood}), and the Damkholer number,

$$Da_{end} = \frac{P_e\,d}{D_{LDL}^{blood}},$$

which is the dimensionless endothelial permeability based on the effective endothelial permeability, P_e. Analysis made by Tarbell (2003) and Hodgson (2002) show that the Da_{end} is much lower than the Sh_d, what implies that the endothelium is the major resistance to LDL transport to the intima.

The last term of equations 1 and 2 represents the LDL oxidation in the intima, which is assumed as an irreversible first order reaction. And, since it was also assumed that all the LDL that goes though the oxidative reaction, LDLox, accumulates in the intima, then $\dot{N}_{LDL} = -k\, C_{LDL}$ is the rate of LDLox accumulation, where k = 1.4x10-4 s-1 is the oxidative reaction rate used by Sun et al (2006).

Last but not least, the LDL flux that goes out of the intima $\left(J_{LDL,out}\right)$ is assumed to leave the intima only in the radial direction toward the media, where the concentration of LDL is assumed to be negligible at a distance of 0.1 mm from the intima. This is based in studies made by other authors (Prosi et al., 2005), who showed that both the value and the gradient of concentration in the media are not sensible to the conditions assumed at the adventitia. The LDL flux leaving the intima is calculated as a diffusive flux $\left(J_{LDL,diff}\right)$ plus a convective flux $\left(J_{LDL,conv}\right)$ as in (5), where γ =1.728 and ϕ = 0.983 are the hindrance and porosity of the intima (assumed constant), $D_{LDL}^{in} = 5\text{x}10^{-14}\, m^2 s^{-1}$ is the diffusion coefficient, and C_{LDL}^{media} is the LDL concentration in the media at a distance δr from the intima (Prosi et al., 2005, Yang and Vafai, 2006):

$$J_{LDL,conv} = \frac{J_v}{\phi}\gamma\, C_{LDL},$$

$$J_{LDL,diff} = -D_{LDL}^{in}\frac{\partial C_{LDL}}{\partial r} \approx -D_{LDL}^{in}\frac{C_{LDL}^{media} - C_{LDL}}{\delta r} \tag{4}$$

Using the model just described, the initial evolution of the concentration of LDL in the intima can be obtained. Not surprisingly, the results obtained in this way predict accumulation of LDL even in zones where it is unlikely, i.e., in the straight portions of the arteries. This is so because the model is still lacking of a sink of LDL due to outflow and due to consumption of cells other than foam cell formation. In this paper, for the sake of simplicity, we just opted for renormalizing the solution by simply subtracting the minimum value from the whole field, so that null or very low growth is predicted in the straight portion of the arteries, as expected.

Finally, once the rate of accumulation of LDLox is obtained, the initial growth rate can be calculated as:

$$\frac{de}{dt} = \frac{V_{LDL}}{M_{LDL}} e_0\, Na\, k\, C_{LDL}, \tag{5}$$

where V_{LDL} is the volume of the LDL molecule, and *Na* is the Avogadro number.

3 COMPUTATIONAL MODEL

Figure 1 shows the carotid bifurcation geometry used for the blood flow simulations. The mesh used had 220901 tetrahedral elements and a parabolic stationary profile with a Re_d of 440 was used as the inlet boundary condition.

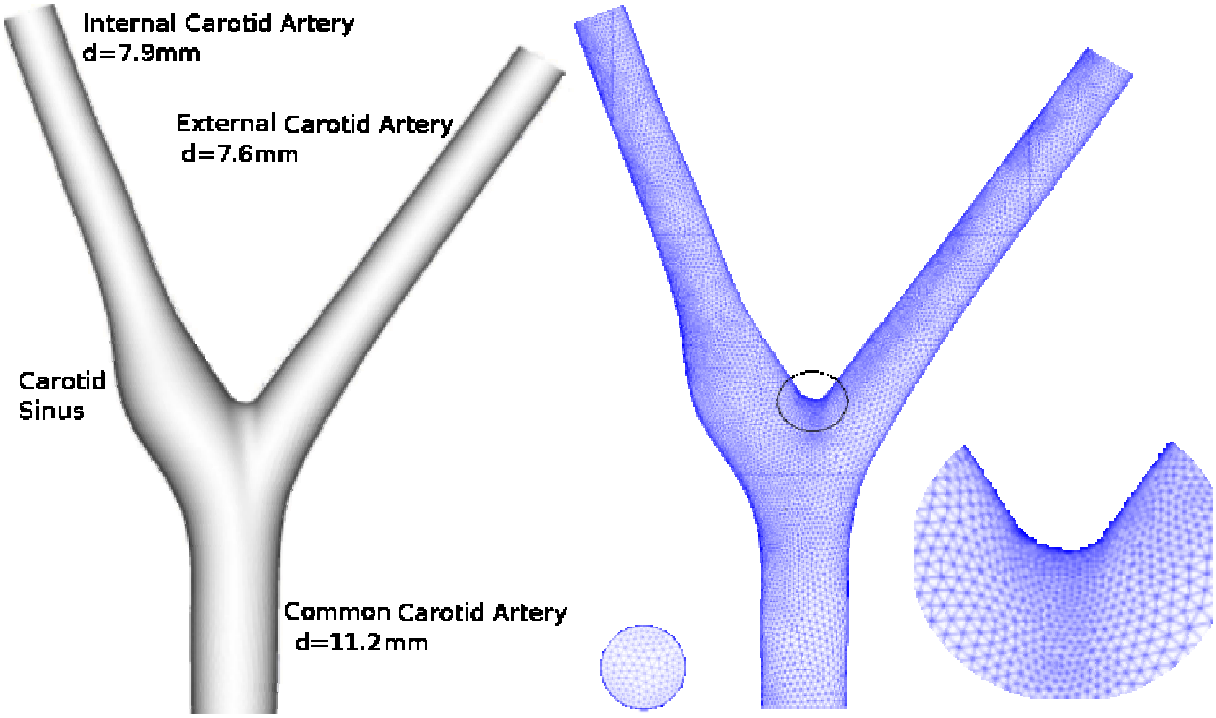

Figure 1: Carotid bifurcation geometry and initial mesh, showing the diameters of the common, external, and internal carotids.

A tension free condition was used as the outlet boundary condition on the internal carotid and a fix parabolic velocity profile was used on the external carotid for the blood flow simulation. The difference in the outlet conditions was to achieve an exit volumetric flow relation of 70:30 between the internal and external carotid arteries. The wall was assumed rigid and impermeable since the blood flow that permeates the endothelium is many orders of magnitude lower that the arterial flow.

The whole model, including the solution of the blood flow, the movement of the mesh, and the prediction of the growth rate of the wall, was implemented using the OpenFOAM library. The boundary wall was moved according to the values given by the growth model, taking small enough time steps to assure the convergence of the moving mesh algorithm and the consistency of the updated mesh. As a reference value for the mesh displacement we took the minimal length of the mesh elements. After each mesh iteration, the fluid was solved for the new mesh using the SIMPLE algorithm, iterating until the steady state is reached.

4 RESULTS

Figure 2 shows the growing of the atheroma with the model we propose. The left side shows the shape of the plaque as the time goes by. The right side shows the plaque for the same time intervals through a cut of the artery at the sinus position, with a cutting plane coplanar with the common carotid entrance.

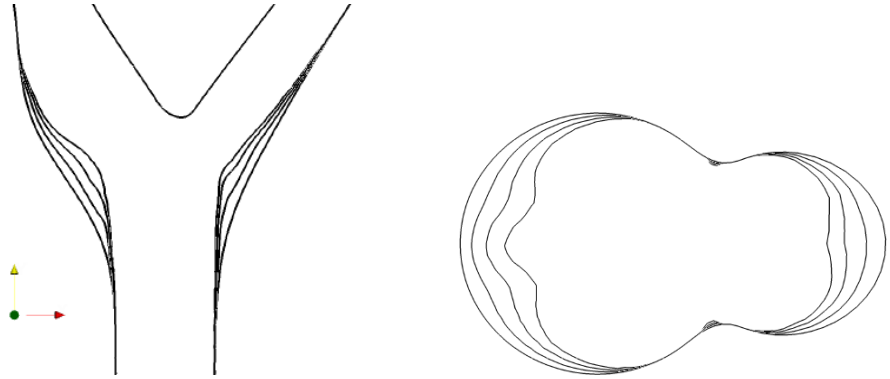

Figure 2: Two views from the growing atheroma. Left, side view of the growth of the atheroma. Right., top view of the growth of the atheroma at a plane coplanar with the inlet and at the bifurcation.

Figure 3 shows the growth rate at the wall for the initial geometry and other three deformed geometries. The red spots show the highest growth rate, spots that seem to disappear as the plaque grows, showing that the model predicts that the atheroma tends to grow slower as it becomes thicker.

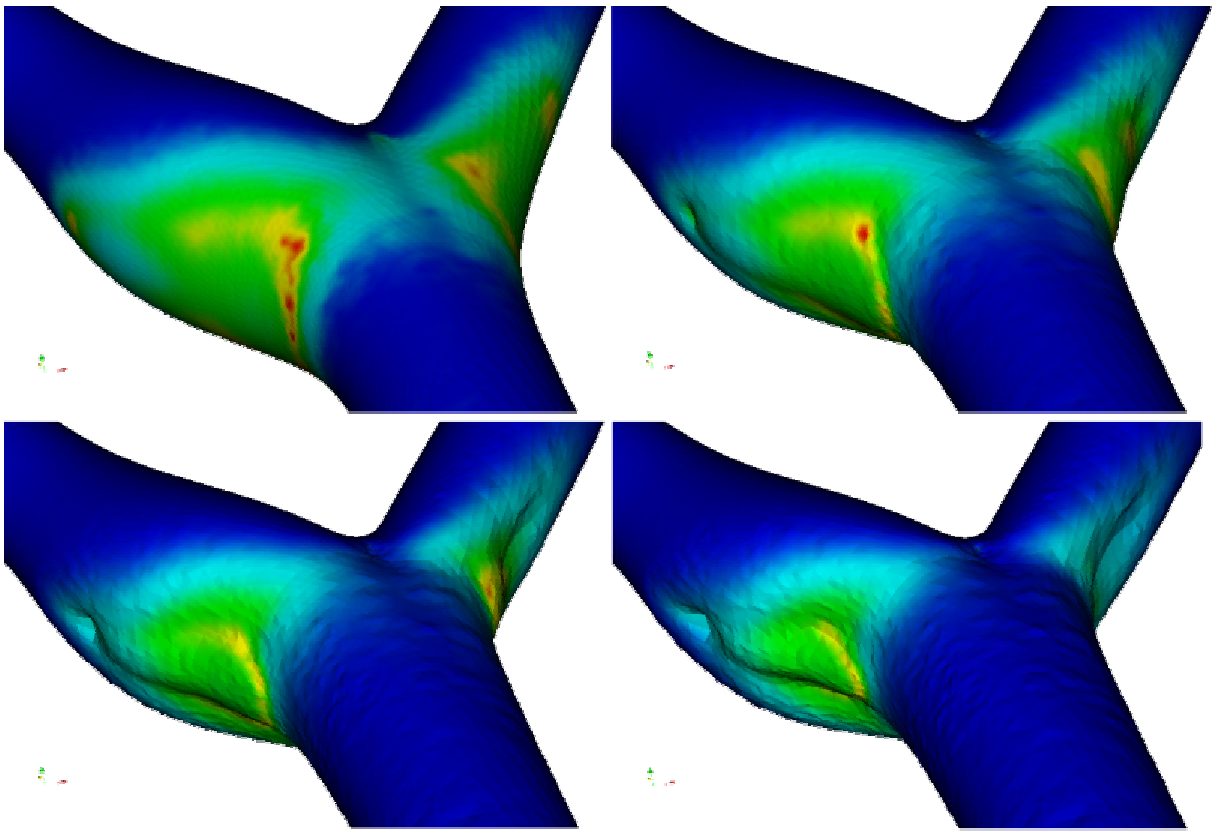

Figure 3: Growth rate at the initial geometry (left) and three deformed geometries. Blue is cero growth and red is the highest growth rate.

Figure 4 shows the streamlines for the initial and the final geometry calculated. The streamlines in the deformed geometry seem to show a less complex flow than the initial one. As the plaque grow the transverse area of the sinus becomes smaller, and so does the external

carotid inlet, and this reduction in area seems to cause the flow to become somewhat smoother and of less “helical” nature.

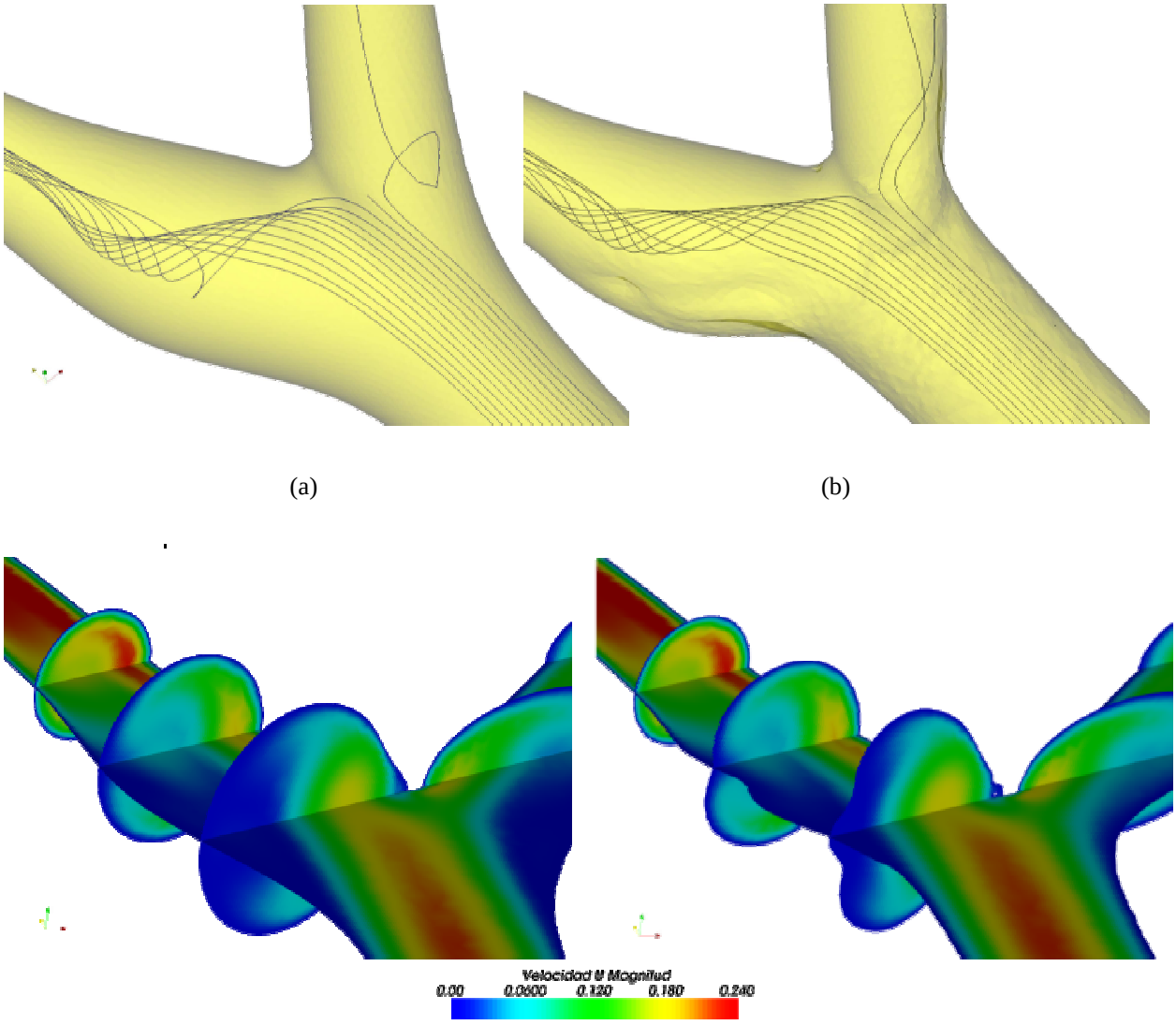

(a) (b)

(c) (d)

Figure 4: Streamlines and velocity modulus for the initial geometry (a, c) and for the deformed geometry corresponding to the latest calculated time (b, d).

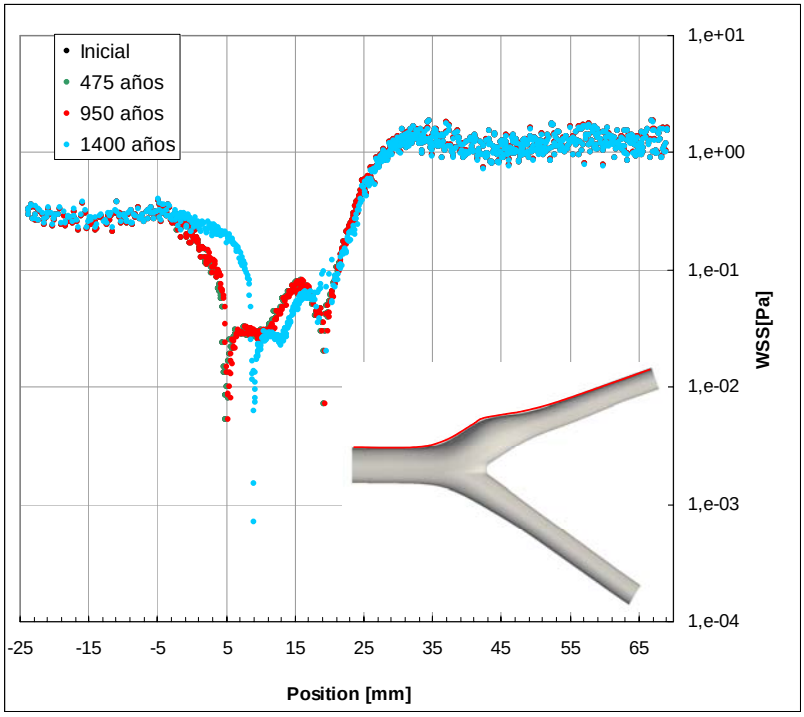

(a)

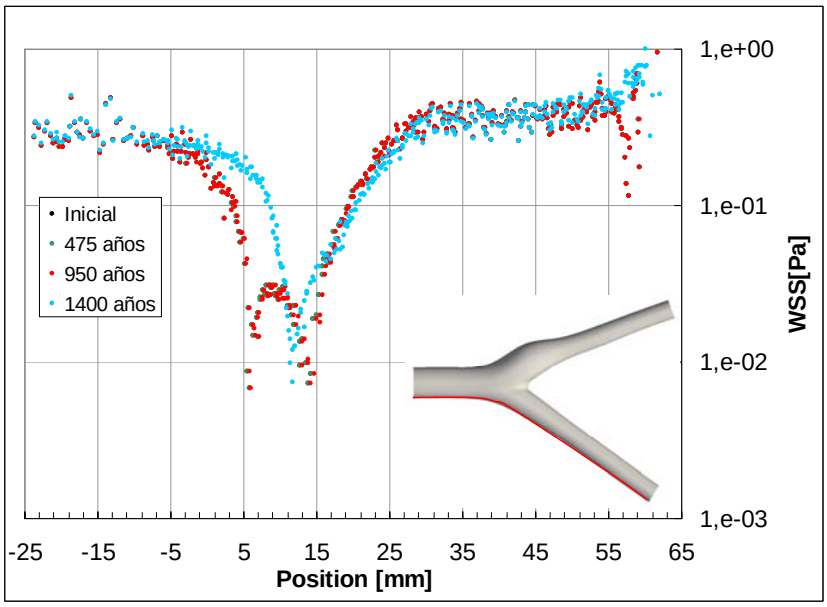

(b)

Figure 5: Wall shear stresses along the external walls of the (a) internal and (b) external carotid arteries, at the central plane of the geometry

Figure 5 (a) and (b) show the wall shear stress along the external walls of the internal and external carotid arteries, at the central plane of the geometry. As it can be seen, the values are in agreement with those obtained by (Ma et al., 1997, Tada and Tarbell, 2006). The values

obtained by Tada and Tarbel (2006) are actually about one order of magnitude higher than ours, and a possible reason for this difference is that they do a pulsatile calculation. As we showed in previous work (Gessaghi et al., 2006), the results of a pulsatile simulation tend to give higher shear stress values at the wall.

The wall shear stress (Fig. 5) on both walls show two points where it reaches local minima. These could be confused with detachment and reattachment points, but we have not seen a closed recirculation area, but instead a helical flow pattern that seems to change direction at those two points. As can be seen, these points tend to move further away from the inlet, and the second point tend to disappear. This is consistent with the results shown in Figure 4, where the streamlines show a less complex flow pattern in the deformed geometry.

The time in years show in the legend were estimated assuming a concentration of blood cholesterol of 1.2 Kg of LDL/m^3 of blood, what explains, together with the fact that there is only accumulation of LDL modeled here, the long times it takes for the plaque to grow.

5 CONCLUSIONS

The numerical results obtained for a carotid bifurcation with a 60º bifurcation angle, assuming blood flow as Newtonian and stationary, predict initial complex helical flow patterns which result in two low velocity and low wall shear stress points on the external walls of both internal and external carotid arteries at the bifurcation region. These two low wall shear stress points are the cause of the higher growth rate predicted by the model presented here. When the years pass the plaque start to form and the wall becomes thicker. Our model predicts a thicker wall at those two points, which delimit a region of low velocities and low wall shear stresses.

It is relevant to mention that there is only one factor included in this model, which is the accumulation of LDL, and the blood LDL concentration was assumed constant. Effects such as concentration polarization, which have been reported previously (Wang et al., 2003), are not considered here. This effect may change the growth rate distribution since the endothelial permeability varies with blood LDL concentration.

REFERENCES

AHA (2003a). Heart diseases and stroke statistics - 2003 update, *www.aha.com*, American Heart Association website

AHA (2003b). International cardiovascular disease statistics, *www.aha.com*, American Heart Association website

Altman, R. (2003). Risk Factors in Coronary Atherosclerosis Athero-Inflammation: The Meeting Point. *Thrombosis Journal*, **1,** 4.

Barakat, A. I. (2001). A model for shear stress-induced deformation of a flow sensor on the surface of vascular endothelial cells. *Journal of Theoretical Biology*, **210,** 221-236.

Barakat, A. I. and Lieu, D. K. (2003). Differential responsiveness of vascular endothelial cells to different types of fluid mechanical shear stress. *Cell Biochemistry and Biophysics*, **38,** 323-344.

Berliner, J. A., Navab, M., Fogelman, A. M., Frank, J. S., Demer, L. L., Edwards, P. A., Watson, A. D. and Lusis, A. J. (1995). Atherosclerosis: Basic Mechanisms : Oxidation, Inflammation, and Genetics. *Circulation*, **91,** 2488-2496.

Braunwald, E., Ziper, D. P. and Libby, P. (2001) In *Heart disease: A textbook of cardiovascular medicine* (Ed), Saunders W.B.C.O, pp. 995-1009.

Caro, C., Fitz-Gerald, J. and Schroter, R. (1971). Atheroma and arterial wall shear. Observation, correlation and proposal of a shear dependent mass transfer mechanism

for atherogenesis. *Proceedings of the Royal Society of London. Series B: Biological Sciences,* **177,** 109-159.
Friedman, M. and Ehrlich, L. (1975). Effect of spatial variations in shear on diffusion at the wall of an arterial branch. *Circulation Research,* **37,** 446-454.
Friedman, M. and Giddens, D. (2005). Blood Flow in Major Blood Vessels: Modeling and Experiments. *Annals of Biomedical Engineering,* **33,** 1710-1713.
Friedman, M. H. and Fry, D. L. (1993). Arterial permeability dynamics and vascular disease. *Atherosclerosis,* **104,** 189-194.
Fry, D. (1969). Certain histological and chemical responses of the vascular interface to acutely induced mechanical stress in the aorta of the dog. *Circulation Research,* **24,** 93-108.
Gessaghi, V. C., Raschi, M. A., Larreteguy, A. E. and Perazzo, C. A. (2005). Simulación del Efecto del LDL en el Crecimiento de una Placa Aterosclerosa. *Mecánica Computacional,* **XXIV**.
Gessaghi, V. C., Raschi, M. A., Larreteguy, A. E. and Perazzo, C. A. (2006). Influencia de las características reológicas y no estacionarias del flujo sanguíneo en un modelo de crecimiento de placas ateroscleróticas. *Mecánica Computacional,* **XXV,** 759-771.
Hazel, A. L., Grzybowski, D. M. and Friedman, M. H. (2003). Modeling the Adaptive Permeability Response of Porcine Iliac Arteries to Acute Changes in Mural Shear. *Annals of Biomedical Engineering,* **31,** 412-419.
Hinderliter, A. and Caughey, M. (2003). Assessing Endothelial Function As a Risk Factor for Cardiovascular Disease. *Current Atherosclerosis Reports,* **5,** 506 - 513.
Hodgson, L. and Tarbell, J. M. (2002). Solute Transport to the Endothelial Intercellular Cleft: The Effect of Wall Shear Stress. *Annals of Biomedical Engineering,* **30,** 936-945.
Jensen-Urstad, K., Jensen-Urstad, M. and Johansson, J. (1999). Carotid Artery Diameter Correlates With Risk Factors for Cardiovascular Disease in a Population of 55-Year-Old Subjects. *Stroke,* **30,** 1572-1576.
Kargol, M. and Kargol, A. (2003). Mechanistic equations for membrane substance transport and their identity with Kedem-Katchalsky equations. *Biophysical Chemistry,* **103,** 117-127.
Ku, D. N. (1997). Blood flow in arteries. *Annual Review of Fluid Mechanics,* **29,** 399-434.
LaMack, J. A., Himburg, H. A., X.M., L. and Friedman, M. H. (2005). Interaction of wall shear stress magnitude and gradient in the prediction of arterial macromolecular permeability. *Annals of Biomedical Engineering,* **33,** 457-464.
Ma, P., Li, X. and Ku, D. N. (1997). Convective mass transfer at the carotid bifurcation. *Journal of Biomechanics,* **30,** 565-571.
Michel, C. C. and Curry, F. E. (1999). Microvascular Permeability. *Physiological Reviews,* **79,** 703-761.
OpenFoam (2007). The Open Source CFD Toolbox, *http://www.opencfd.co.uk/openfoam/*, OpenCFD Ltd
Prosi, M., Zunino, P., Perktold, K. and Quarteroni, A. (2005). Mathematical and numerical models for transfer of low-density lipoproteins through the arterial walls: a new methodology for the model set up with applications to the study of disturbed lumenal flow. *Journal of Biomechanics,* **38,** 903-917.
Rappitsch, G. and Perktold, K. (1996). Computer simulation of convective diffusion processes in large arteries. *Journal of Biomechanics,* **29,** 207-215.
Ross, R. (1999). Atherosclerosis -- An Inflammatory Disease. *New England Journal of Medicine,* **340,** 115-126.

Stangeby, D. and Ethier, C. (2002). Computational analysis of coupled blood-wall arterial LDL transport. *Journal of Biomechanical Engineering,* **124,** 1-8.

Sun, N., Wood, N., Hughes, A., Thom, S. and Xu, X. (2006). Fluid-Wall Modelling of Mass Transfer in an Axisymmetric Stenosis: Effects of Shear-Dependent Transport Properties. *Annals of Biomedical Engineering,* **31,** 1-10.

Tada, S. and Tarbell, J. (2006). Oxygen Mass Transport in a Compliant Carotid Bifurcation Model, Vol. 34, pp. 1389-1399.

Tarbell, J. (2003). Mass transport in arteries and the localization of atherosclerosis. *Annual Review of Biomedical Engineering,* **5,** 79-118.

Wang, G., Deng, X. and Guidoin, R. (2003). Concentration polarization of macromolecules in canine carotid arteries and its implication for the localization of atherogenesis. *Journal of Biomechanics,* **36,** 45-51.

Yang, N. and Vafai, K. (2006). Modeling of low-density lipoprotein (LDL) transport in the artery--effects of hypertension. *International Journal of Heat and Mass Transfer,* **49,** 850-867.